701352

LA-3365-MS

81

LOS ALAMOS SCIENTIFIC LABORATORY

LOS ALAMOS [redacted] of the [redacted] NEW MEXICO

University of California

Some Biological Aspects of Radioactive Microspheres

LANL

UNITED STATES
ATOMIC ENERGY COMMISSION
CONTRACT W-7405-ENG. 36

0005276

LEGAL NOTICE

This report was prepared as an account of Government sponsored work. Neither the United States, nor the Commission, nor any person acting on behalf of the Commission:

A. Makes any warranty or representation, expressed or implied, with respect to the accuracy, completeness, or usefulness of the information contained in this report, or that the use of any information, apparatus, method, or process disclosed in this report may not infringe privately owned rights; or

B. Assumes any liabilities with respect to the use of, or for damages resulting from the use of any information, apparatus, method, or process disclosed in this report.

As used in the above, "person acting on behalf of the Commission" includes any employee or contractor of the Commission, or employee of such contractor, to the extent that such employee or contractor of the Commission, or employee of such contractor prepares, disseminates, or provides access to, any information pursuant to his employment or contract with the Commission, or his employment with such contractor.

All LA...MS reports are informal documents, usually prepared for a special purpose and primarily prepared for use within the Laboratory rather than for general distribution. This report has not been edited, reviewed, or verified for accuracy. All LA...MS reports express the views of the authors as of the time they were written and do not necessarily reflect the opinions of the Los Alamos Scientific Laboratory or the final opinion of the authors on the subject.

Printed in USA. Price $3.00. Available from the Clearinghouse for Federal Scientific and Technical Information, National Bureau of Standards, United States Department of Commerce, Springfield, Virginia

LANL

0005277

LA-3365-MS
UC-41, HEALTH
AND SAFETY
TID-4500 (43rd Ed.)

LOS ALAMOS SCIENTIFIC LABORATORY
LOS ALAMOS [redacted] of the [redacted] NEW MEXICO
University of California

Report written: July 20, 1965

Report distributed: August 23, 1965

Some Biological Aspects of Radioactive Microspheres

by

Biological and Medical Research Group

LANL

0005278

ABSTRACT

The nature of the potential hazards produced by atmospheric reentry and destruction of space nuclear power systems will be influenced by the size of particles returning to the earth's surface. Fine particles (less than ~10 μ) will be more widely dispersed but will be in the respirable size range, with the possibility of entering the exchange space of the lung where biological elimination is relatively quite slow. Larger particles will be less widely dispersed but will constitute more intense discrete radiation sources. The size of particles reaching the earth's surface will depend on the method of system destruction. As regards potential hazard control, the method of choice will depend on a number of factors, among which are the biological effects which may be produced by radioactive particles too large to be inhaled. This report covers some preliminary observations believed pertinent to assessing the biological effects of particulate radiation sources, particularly fissioned $^{235}UC_2$ microspheres in the size range of about 100 to a few hundred μ.

LANL

0005279

All pyrocarbon-coated $^{235}UC_2$ particles and about 85 percent of uncoated ones appeared to maintain their integrity for 24 hours in gastric juice. Mean transit time of uncoated spheres through the gastrointestinal tract of 57 normal adults was 34.5 $\pm$ 16.6 hours. Their high density ($\sim$ 10.8) does not seem to be a factor in rate of passage. When placed in situ, uncoated particles underwent disintegration and solubilization in 4 to 6 weeks; coated ones were still partially intact at 8 to 12 weeks. The disintegration process involved encapsulation, fibroblastic infiltration of the particle mass and, in case of the coated particles, vigorous macrophage ingestion of carbon.

Emergent beta-ray spectra of fissioned spheres were measured and dose as a function of depth in the skin calculated and compared with measured dose using photographic emulsion dosimetry. Calculated values (based on exponential absorption) were approximately 20 percent higher than measured values.

Lesions produced on the skin of the backs of monkeys by calculated beta-ray doses (of 1300 to 52,000 rads) from fissioned spheres were examined grossly and microscopically. Doses above about 10,000 rads produced small areas of erythema which persisted for 3 weeks. Microscopically, these lesions at 6 weeks post exposure appeared of little medical importance, although both dermal and epidermal changes were discernible.

LANL

0005280

ACKNOWLEDGMENTS

We wish to express our appreciation to L. D. P. King of the Laboratory's Rover Flight Safety Office for his support and encouragement and to R. J. Bard, Group Leader of CMB-8, for supplying the $^{235}UC_2$ microspheres. We are grateful to Dr. C. C. Lushbaugh of the Medical Division, Oak Ridge Institute of Nuclear Studies, who helped with the pathology interpretation of biopsy material.

LANL

0005281

CONTENTS

		Page
	Abstract	3
	Acknowledgments	5
CHAPTER I	Introduction	11
CHAPTER II	Integrity of $^{235}UC_2$ Microspheres in Gastric Fluids	13
CHAPTER III	Gross Gastrointestinal Transit Time of Low- and High-Density Microspheres in Man	21
CHAPTER IV	Reaction and Fate of Interstitially Placed Graphite-Coated and Uncoated $^{235}UC_2$ Microspheres	31
CHAPTER V	Emergent Beta-Ray Spectrum of Fissioned $^{235}UC_2$ Microspheres and Calculation of Beta Radiation Depth-Dose in Tissue	42
CHAPTER VI	Measurement of Beta-Ray Dose at the Average Depth of the Basal Layer of the Skin from Fissioned $^{235}UC_2$ Microspheres in Contact with the Skin Surface	51
CHAPTER VII	Observations of Acute Radiation Effects from Fissioned $^{235}UC_2$ Microspheres in Contact with the Skin Surface	58

LANL

0005282

TABLES

		Page
Table II-1	Weight and Diameter of Carbon-Coated $^{235}UC_2$ Microspheres before and after 24-hour Immersion in Primate Gastric Juice	17
Table II-2	Particle Diameter of Uncoated $^{235}UC_2$ Microspheres before and after 24-hour Immersion in Primate Gastric Juice	19
Table III-1	Gross Gastrointestinal Transit Times for Small Particles of Different Densities in Man	25
Table III-2	Gross Gastrointestinal Transit Times for Small Particles of Different Densities in Man	27
Table V-1	Calculated Beta Radiation Doses from Fissioned $^{235}UC_2$ Microspheres	48
Table V-2	Calculated Beta Radiation Doses from Fissioned $^{235}UC_2$ Microspheres used in Skin Exposure Studies	48
Table VI-1	Calculated and Measured Beta Radiation Dose from Activated $^{235}UC_2$ Microspheres	57
Table VII-1	Estimated Beta Radiation Doses to Basal Layer of the Skin (100 μ in Depth) from Fissioned $^{235}UC_2$ Microspheres	61

LANL

0005283

ILLUSTRATIONS

		Page
Figure II-1	Sectioned UHTREX particle showing $^{235}UC_2$ kernel and duplex coating of laminar and columnar pyrocarbon	15
Figure III-1	Gamma-ray spectrum of human fecal sample showing photopeaks at ~ 170 kev (^{235}U) and at ~ 840 kev (^{54}Mn) from ingested microspheres	24
Figure III-2	Gross transit time in relation to time of day particles were ingested	29
Figure IV-1	Hairless mouse with two carbon-coated $^{235}UC_2$ beads as placed subcutaneously 26 days prior to photograph	34
Figure IV-2	Subcuticular implant of microsphere after 8 weeks	35
Figure IV-3	Encapsulated microspheres removed from the peritoneum of a rat 8 weeks after implant	37
Figure IV-4	Intraportally implanted microspheres (carbon-coated) after (A) 8 weeks, and (B) 12 weeks in situ	39
Figure V-1	Four-pi beta-ray spectrometer	44

LANL

0005284

		Page
Figure V-2	Beta-ray spectrum of ^{137}Cs source as measured with a 4π beta-ray spectrometer	45
Figure V-3	Experimental ^{235}U fission product beta decay spectra at four times after fission	46
Figure V-4	Calculated beta radiation depth-dose profile in percent of the dose at a depth of 100 μ, assuming exponential absorption	49
Figure VI-1	Skin mockup for film dosimetry of $^{235}UC_2$ microspheres	53
Figure VI-2	Measured and calculated lateral beta-ray dose distribution at 100 μ below the surface from an activated $^{235}UC_2$ microsphere (160 μ in diameter)	55
Figure VII-1	Method of placing microspheres (A), and exposure grid system (B)	62
Figure VII-2	Pictorial record of the 52,100-rad lesion at (A) 7 days, (B) 14 days, (C) 21 days, and (D) 28 days post exposure	65

LANL

0005285

CHAPTER I

INTRODUCTION

Assessment of the potential hazards of inspired radioactive aerosols poses perhaps the most complex and difficult health protection problem facing the nuclear energy industry. Atmospheric reentry and burnup of nuclear rocket propulsion reactors and auxiliary power supplies will create potential radioactive particle inhalation hazards specifically affecting the use of nuclear energy in space missions. One possibility of alleviating the potential inhalation hazard is to control the size of the radioactive particles returning to the earth's surface such that they will not be in the respirable size range or at least above the size range that may enter the exchange space of the lungs (larger than $\sim 10\ \mu$), where the removal rate is relatively quite slow. In toto the problem is, of course, not that simple. The larger the particle size, the fewer will be their number and the lower will be the probability that a specific individual or group

LANL

0005286

will be exposed to one or more particles. The larger the particles, however, the more confined will be their distribution, the higher the gross radiation intensity per unit area, and the greater the radioactivity per particle because of both size and shorter decay time as a consequence of their more rapid rate of fall. Whether control of reentry particle size lessens the potential hazards of space applications of nuclear energy depends on evaluation of all of these parameters in relation to the biological effects produced by radioactive particles too large to enter the respiratory tract. If insoluble, such particles may constitute discrete sources of alpha, beta, or gamma radiation or mixed sources of these radiation types. Discrete sources deposited on the skin surface may produce significant radiation lesions and if swallowed will result in irradiation of the gastrointestinal mucosa. If soluble, the radioisotopes present may be absorbed directly into the body or enter the ecological cycle and constitute a potential internal radiation source. The latter problem may be circumvented by employing only highly insoluble materials for space applications. This report covers some preliminary observations believed pertinent to assessing the biological effects of discrete radiation sources, particularly activated or fissioned $^{235}UC_2$ microspheres in the size range of about 100 to a few hundred μ.

LANL

0005287

CHAPTER II

INTEGRITY OF $^{235}UC_2$ MICROSPHERES IN GASTRIC FLUIDS

(C. R. Richmond and J. E. London)

Consideration of radiation dose from discrete radioactive particles temporarily residing within the lumen of the gastrointestinal tract requires knowledge of particle integrity, solubilization, and assimilation by the body. If particle integrity is not maintained in body fluids, then solubilization and assimilation may assume primary importance. The following tests were performed to assess the degree of $^{235}UC_2$ particle integrity during controlled exposure to gastric juice.

Integrity of Carbon-Coated $^{235}UC_2$ Particles

Integrity of UHTREX* particles, consisting of a $^{235}UC_2$ kernel surrounded by a duplex layer of laminar and columnar

*Acronym for Ultra High Temperature Reactor EXperiment.

LANL

0005288

pyrocarbon (Fig. II-1), in monkey gastric juice was investigated. The density of the particles was 2.6, and the uranium content was about 30.36 percent. Each of 12 particles was carefully weighed and measured (diameter) before and after being placed into monkey gastric juice for 24 hours. This time period was selected as it would almost certainly exceed the maximum time a particle would remain in the acid environment of the stomach. It was assumed also that the acidic conditions of the stomach would be the most detrimental to the particles. The gastric fluid was obtained from anesthetized monkeys (Macaca speciosa) some 30 minutes after the first meal following an overnight fast. Particulate materials were removed from the juice by filtration through a very coarse fritted glass filter. If necessary, the filtered juice was adjusted to pH 3.5 with HCl. Each particle was placed in 3 to 5 ml of the filtered gastric fluid contained in a plastic receptacle. The contents of the receptacle were maintained at 37°C with continuous agitation throughout the 24-hour test period.

Particle diameter measurements were made with a Vickers-A.E.I. image-splitting device attached to a standard binocular light microscope. Calibration of the optical system was achieved by using a stage-mounted 100-μ graticule marked at 2-μ intervals. Each particle was measured five consecutive

LANL

0005289

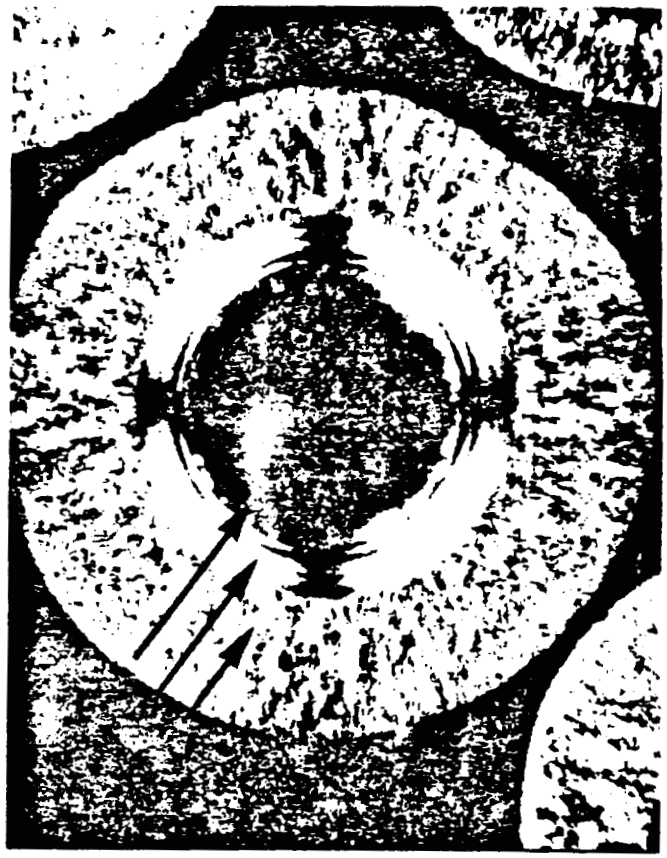

Fig. II-1. Sectioned UHTREX particle showing $^{235}UC_2$ kernel and duplex coating of laminar and columnar pyrocarbon.

LANL

0005290

times, removed from the slide, and then remeasured five additional times. Mass measurements were made with a Cahn microbalance with a known accuracy and precision of about 2 μg.

Table II-1 shows particle weights and diameters before and after immersion for 24 hours in gastric juice. No real diameter and mass changes were apparent, and all differences were within the known measurement errors. The maximum differences observed were in diameter and were on the order of 2 to 4 percent of the initially observed value. Very probably the differences are not real but merely a reflection of the relative position of the particle during each set of measurements before and after immersion. Thus, as a first approximation, clad UHTREX particles maintain their integrity when agitated in warmed primate gastric juice for 24 hours. No fracturing, pitting, or erosion was observed.

Integrity of Uncoated $^{235}UC_2$ Particles

The integrity of uncoated $^{235}UC_2$ particles in gastric fluid was investigated also, since rupture of the pyrocarbon coating conceivably could result in exposure to the bare $^{235}UC_2$ kernel. Because of the low mass (20 to 50 μg) and attendant problems in handling uncoated $^{235}UC_2$ particles, only diameter measurements were made routinely. Otherwise, the experimental protocol given in the previous section was

LANL

0005291

TABLE II-1. WEIGHT AND DIAMETER OF CARBON-COATED $^{235}UC_2$ MICROSPHERES BEFORE AND AFTER 24-HOUR IMMERSION IN PRIMATE GASTRIC JUICE

Trial No.	Weight (μg)		Diameter (μ)	
	Pre	Post	Pre	Post
1	70	71	377.9	380.4
2	61	60	370.5	362.6
3	83	82	383.6	389.7
4	86	86	391.8	393.7
5	90	91	392.8	402.3
6	62	61	359.8	367.0
7	62	62	359.0	354.8
8	60	58	360.8	362.7
9	120	118	433.6	438.3
10	105	105	408.2	414.2
11	83	82	390.1	389.9
12	87	87	401.4	397.9

LANL

0005292

duplicated, except particle density in this case was about 10.8. Preliminary observations indicated that uncoated $^{235}UC_2$ particles were considerably less spherical than were coated ones. Repositioning a particle between successive measurements introduced a total error of about 5 percent for the diameter value. Table II-2 lists the measured diameters obtained from 26 particles before and after immersion in primate gastric juice for 24 hours. Differences exceeding 5 percent are shown in column 4. In trial No. 20, the particle was completely fractured into two roughly equal halves which were still mutually connected. In three other trials, the diameters after immersion were from 10 to 20 percent smaller than the originally observed values. Because of diameter-volume relations, a difference of ~ 20 percent (trial No. 14) in diameter measurement represents a decrease by a factor of 2 in the volume and hence cannot be ignored. A 5 percent decrease in diameter represents a reduction in volume of ~10 percent. Observation of uncoated $^{235}UC_2$ particles not used in this study showed the presence of numerous surface imperfections. It is not unreasonable to assume that similar particles might have inadvertently been used in this study, as it is extremely difficult to observe the entire surface of a small particle of this nature. Regardless of the cause, it appears that uncoated $^{235}UC_2$ particles are

LANL

0005293

TABLE II-2. PARTICLE DIAMETER OF UNCOATED $^{235}UC_2$ MICROSPHERES BEFORE AND AFTER 24-HOUR IMMERSION IN PRIMATE GASTRIC JUICE

Trial No.	Diameter (μ)		Difference (percent)*
	Pre	Post	
1	203.1	212.2	
2	178.0	179.3	
3	211.8	214.0	
4	166.9	167.1	
5	211.4	171.7	-18.8
6	200.3	203.7	
7	215.1	216.0	
8	175.0	175.2	
9	160.2	163.6	
10	164.5	164.1	
11	186.1	167.3	-10.1
12	165.3	159.2	
13	164.2	166.5	
14	173.5	136.3	-21.4
15	159.3	158.6	
16	165.5	165.5	
17	186.0	185.3	
18	177.3	175.2	
19	154.9	154.5	
20	155.9	Fractured	Fractured
21	152.1	151.1	
22	171.5	167.7	
23	168.3	171.4	
24	137.9	138.5	
25	162.5	162.1	
26	137.6	138.6	

*If greater than 5 percent of the initial value.

LANL

0005294

less able to maintain their integrity for 24 hours in gastric juice. Still, in 85 percent of the cases, the small changes in particle diameter were judged to fall within experimental error.

LANL

0005295

CHAPTER III

GROSS GASTROINTESTINAL TRANSIT TIME OF LOW- AND HIGH-DENSITY MICROSPHERES IN MAN

(C. R. Richmond and J. E. Furchner)

Estimates of the radiation dose incurred from the passage of small radioactive particles through the gastrointestinal tract depend on a number of physical and biological factors. Included among the latter is the time spent by the particle during passage through the gastrointestinal tract (referred to hereafter as gross transit time). Estimates for gross transit time for small (100- to 200-μ) high-density particles have been purely speculative. Possible density effects on entrapment between villi or movement against gravity (e.g., up the ascending colon or out from the gastric fundus) have been suggested as mechanisms that might result in long retention times. In addition, the great variability in defecation habits among people augments the lack of agreement on the average time required for any material to pass through the gastrointestinal tract. The purpose of this study

LANL

0005296

was to measure gross transit times of low- and high-density microspheres (~100 to 200 μ in diameter) in a small sample of normal adults.

Methods

Two kinds of particles were used: ceramic microspheres 149 ± 11 μ in diameter having a density of 3.0 g/cm^3* and containing approximately 150 picocuries (pCi) ^{54}Mn per sphere, and uncoated $^{235}UC_2$ spheres 173 ± 39 μ in diameter having a density of ~ 10.8 g/cm^3. One ceramic sphere and two $^{235}UC_2$ spheres were easily detectable and differentiated in a fecal sample when measured for 30 minutes in a thin-window, NaI (Tl), twin-crystal counter operated with a 400-channel pulse-height analyzer (1). Because of the very small amounts of material, the low specific activity of ^{235}U and the gamma-ray positron emission decay of ^{54}Mn, the calculated radiation dose delivered the segments of the gastrointestinal tract were extremely low, even for very long residence times in the lower large intestine, and far below ($^{235}U \sim 10^{-4}$, $^{54}Mn \sim 10^{-6}$) accepted maximum permissible levels for these materials (2).

Experimental protocol was as follows. A gelatin capsule containing two $^{235}UC_2$ spheres and one ^{54}Mn-labeled sphere was

---

*Obtained from 3-M Company, St. Paul, Minn.

LANL

0005297

measured for 30 minutes in the twin-crystal spectrometer. This was done to verify the presence of peaks at about 180 and 840 kev in the gamma-ray spectrum. Occasionally non-labeled or very weakly labeled ^{54}Mn spheres were encountered and were not used. Each person was given a capsule containing a set of measured spheres and instructed to collect each succeeding fecal sample until the particles were recovered. Times of ingestion and sample voiding were recorded. One person repeated the test 10 different times to provide an estimate of variation within the same individual. Several others repeated the ingestion at different times of the day to provide an estimate of the time-of-day variable. Information was obtained on 57 individuals and represents the history of some 156 separate particles (114 $^{235}UC_2$- and 42 ^{54}Mn-labeled ceramic spheres).

Results and Discussion

Figure III-1 shows the gamma-ray spectrum obtained from a measurement of a fecal sample voided by one subject about 24 hours after swallowing the particles. Both peaks are easily distinguishable.

Table III-1 gives details of gastrointestinal passage for each of the 52 subjects who passed particles of both densities in the same sample. Mean gross transit time was

LANL

0005298

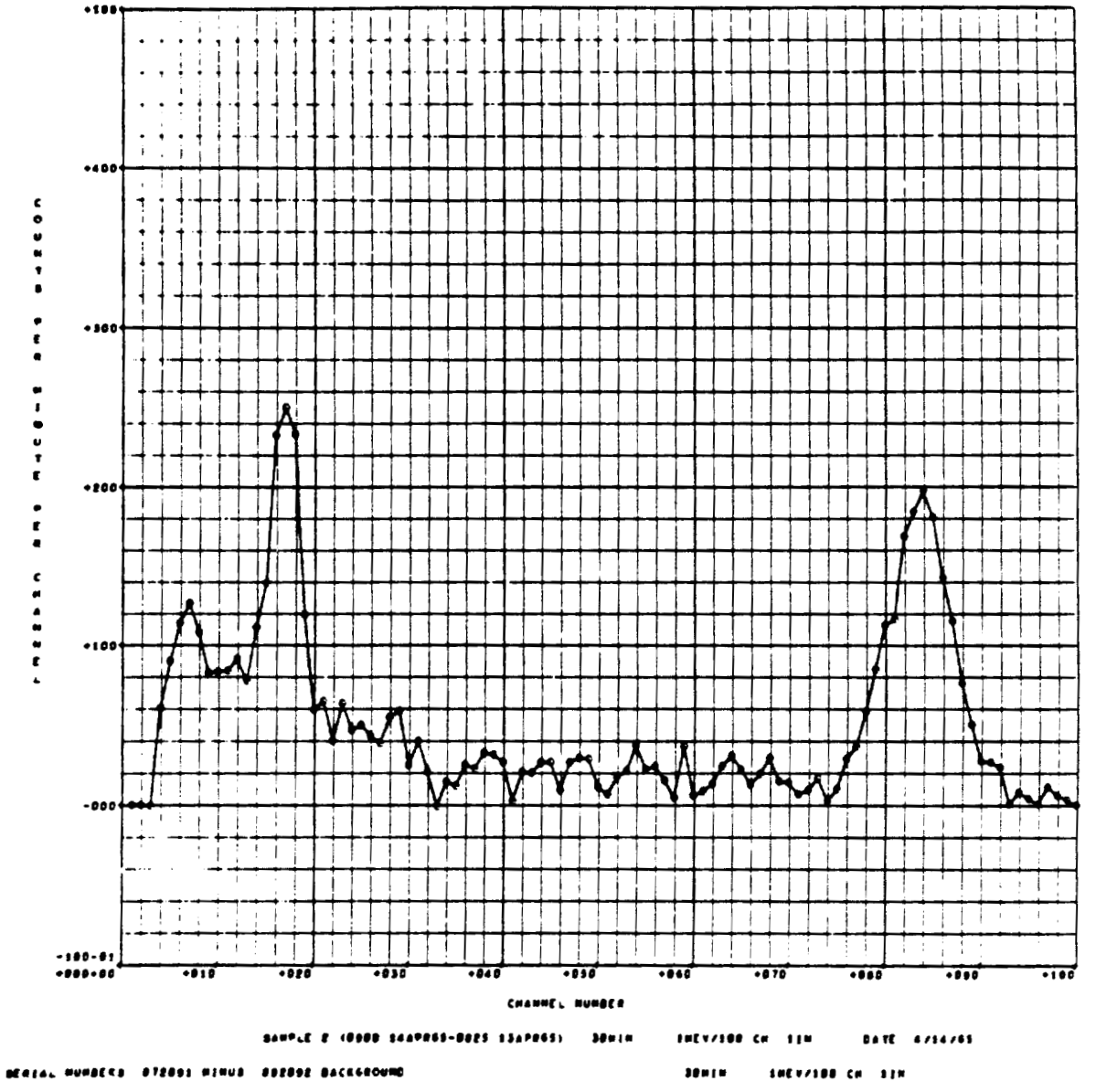

Fig. III-1. Gamma-ray spectrum of human fecal sample showing photopeaks at ~180 kev (^{235}U) and at ~840 kev (^{54}Mn) from ingested microspheres.

LANL

0005299

TABLE III-1. GROSS GASTROINTESTINAL TRANSIT TIMES FOR SMALL PARTICLES OF DIFFERENT DENSITIES IN MAN

Subject	G.T.T.* (hours)	Sample No.	Subject	G.T.T.* (hours)	Sample No.
1	31.4	2	27	53.3	1
2	15.5	1	28	45.3	2
3	27.6	2	29	71.5	3
4	22.3	1	30	23.0	1
5	39.5	2	31	71.3	3
6	14.0	3	32	31.2	4
7	29.3	2	33	46.0	3
8	26.1	1	34	43.4	1
9	61.3	3	35	17.2	1
10	58.0	3	36	49.3	3
11	55.1	3	37	22.2	2
12	35.3	3	38	68.2	3
13	23.3	1	39	16.2	1
14	27.4	3	40	22.5	2
15	41.0	2	41	28.1	2
16	17.4	1	42	20.3	1
17	33.3	2	43	56.3	2
18	24.5	1	44	18.4	1
19	38.0	2	45	18.5	1
20	48.0	1	46	35.0	2
21	34.3	2	47	17.5	1
22	41.3	2	48	27.3	2
23	72.0	4	49	41.0	2
24	22.4	2	50	24.6	2
25	22.5	1	51	25.8	2
26	20.4	2	52	24.3	2

*Gross transit time.

LANL

0005300

34.5 hours, with a standard error of 16.6 hours. This value is in good agreement with the value of 31 hours recommended for the standard man by Committee II of the International Commission on Radiological Protection (2). LeRoy and co-workers (3) recently suggested a revision to 49 hours; this value appears to be large for a representative average for discrete particles. Individual values ranged from 14.0 to 95.6 hours, or about 7 fold. The minimum value was obtained for a normal stool sample and did not represent a diarrheal condition. Most probably the gross transit time values do not correspond to a normal distribution.

On the average, particles were passed in the second fecal sample following ingestion; the range was from 1 to 5. An occasional individual forgot to collect one or more fecal samples after ingesting the spheres. In these cases the results were discarded from the study.

In only 5 of the 57 trials were the two types of particles separated and passed in different stools; 3 subjects passed the lower density ceramic spheres first, and 2 subjects passed the higher density $^{235}UC_2$ spheres first. Table III-2 shows data for the 5 trials, representing about 9 percent of the sample. Gross transit time may be expected to depend on time of particle ingestion with respect to the next regular bowel movement, especially in individuals with regular habits.

LANL

0005301

TABLE III-2. GROSS GASTROINTESTINAL TRANSIT TIMES FOR SMALL PARTICLES OF DIFFERENT DENSITIES IN MAN

	^{54}Mn Ceramic Spheres		$^{235}UC_2$ Spheres	
Subject	G.T.T.* (hours)	Sample No.	G.T.T.* (hours)	Sample No.
53	28.5	3	51.8	4
54	21.5	2	51.5	3
55	70.9	3	47.1	2
56	74.5	4	95.6	5
57	32.0	2	23.5	1

*Cross transit time.

LANL

0005302

Figure III-2 shows trials in 3 individuals relating gross transit time and time of day the particles were ingested. In each parenthesis is shown the ingestion time and sample number of the stool containing the radioactivity. The steady decrease in gross transit time noted in the first 4 trials for individual A represents decreasing times between particle ingestion and early morning bowel emptying. However, trial 5 shows that when particles were ingested at 1700 hours they were not passed the following morning but rather on the second morning following ingestion. Individual B shows a similar pattern for three trials spaced at 6-hour intervals. Individual C, representing 10 trials, is typical of a person with non-regular bowel habits. However, in most cases the activity was identified in the second sample and most values fell within a factor of 2.

Experiments designed to measure differential transit times of small particles through the gastrointestinal tract of rodents and dogs are in progress. Hopefully, these data may be used to derive values applicable to man through correlations of differential and gross transit times and anatomical characteristics of the gastrointestinal tract.

Although only gross transit times were observed in this study and the sample size was relatively small, density of ingested particles does not seem to influence rate of passage

LANL

0005303

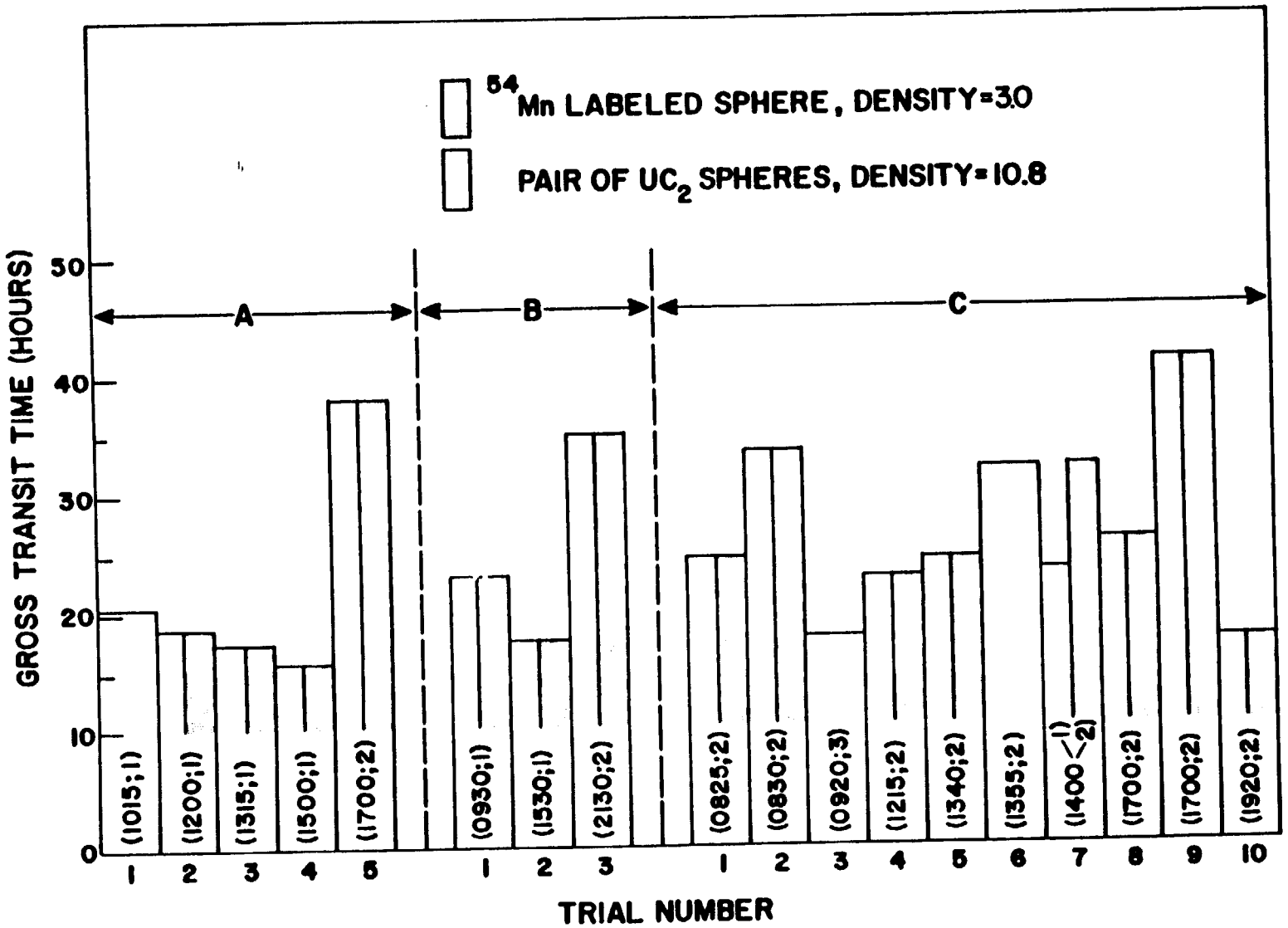

Fig. III-2. Gross transit time in relation to time of day particles were ingested.

LANL

0005304

through the gastrointestinal tract of normal healthy adults. There was no indication of greater than expected holdup of microspheres in the digestive system. All spheres were accounted for in 96 hours after ingestion. Mean gross transit time was 34.5 hours, with a standard error of 16.6 hours. Most probably gross transit time values do not correspond to a normal distribution and the bowel movement habits of the individual are the dominant factor.

REFERENCES

(1) M. J. Fulwyler, Los Alamos Scientific Laboratory Report LA-3132-MS (1964), p. 142.

(2) Report of Committee II on Permissible Dose for Internal Radiation, in: Recommendations of the International Commission on Radiological Protection, Pergamon Press, London (1959).

(3) G. V. LeR[illegible] J. H. [illegible] and [illegible] Hasterlik, Argonne Cancer Research Hospital Report ACRH-102 (1965), 32 p.

LANL

0005305

CHAPTER IV

REACTION AND FATE OF INTERSTITIALLY PLACED GRAPHITE-COATED AND UNCOATED $^{235}UC_2$ MICROSPHERES

(J. C. Hensley)

The reaction and fate of interstitially located carbon-coated and uncoated $^{235}UC_2$ microspheres may have bearing on the public health hazard imposed by such particles in the event of nuclear reactor reentry and destruction. Atmospheric terminal velocity calculations indicate that particles in the 100- to 200-μ diameter range would not penetrate the squamous epithelial tissue. However, particle deposition in broken skin areas, in the medial or lateral canthus of the eye, the internal auditory meatus, or even the mouth with possible tissue reaction to the radioactivity might ultimately result in interstitial incorporation. An indication of response of tissue to the microspheres and effect of tissue and tissue fluids on the particles may be of interest.

LANL

0005306

Methods and Results

Three types of spheres were used: graphite-coated and uncoated $^{235}UC_2$ spheres and spheres of $^{239}PuO_2$. The latter were used to try to differentiate normal tissue reaction to relatively nonradioactive particles from reaction to highly radioactive particles (in this case, intense alpha radiation). Microspheres of about 100- to 300-μ diameter were implanted subcutaneously or intradermally, intraperitoneally, and intraportally.

Subcutaneous or Intradermal Implants

Five particles of each type were implanted intradermally on the backs of each of 4 Macaca speciosa monkeys (previously prepared with 1-cm tatooed grids). In all cases the particles were placed by means of a properly sized hypodermic needle and stylet. When the needle (with bevel up) was properly positioned in the desired skin layer, the bead was carefully pushed from and about 5 mm ahead of the needle tip (parallel to the skin surface) with the stylet.

Gross observations of degree of inflammation were made routinely for 90 days. Other than the initial inflammation along the implant tract, no reaction to the coated and uncoated $^{235}UC_2$ spheres could be observed grossly at 6 days post implant. The $^{239}PuO_2$ spheres, however, elicited grossly

LANL

0005307

prominent reactions for 6 to 8 weeks. After this period the majority of uncoated beads (including $^{239}PuO_2$) were no longer visible. Dispersed carbon from the coated beads, however, was readily visible at this time. Detailed information on the fate and reaction of these materials placed intradermally on the backs of monkeys will require histological examination of biopsy samples.

Graphite-coated and uncoated $^{235}UC_2$ spheres were also placed subcutaneously in intermittent hairless mice. The hairless strain (developed in this Laboratory) was used to facilitate gross observations of tissue response. Figure IV-1 shows one of these mice with two subcutaneously implanted beads (graphite-coated) 26 days after implant. Some dispersion of the graphite from the particle can be seen at this time. As would be expected, the rate of dissolution of bare $^{235}UC_2$ spheres was more rapid than for coated spheres. Disintegration of the uncoated spheres was well underway by 4 to 5 weeks and was complete by about 8 weeks. Disintegration of the graphite-coated particles seemed initially to be quite selective (i.e., only an occasional particle seemed subject to the tissue effect). After about 12 weeks, however, little evidence of the spheres could be seen grossly. Serial histosections through a coated microsphere implanted subcutaneously for 8 weeks are shown in Fig. IV-2. This figure shows fibroblastic infiltration into the mass of the microsphere

LANL

0005308

Fig. IV-1. Hairless mouse with two carbon-coated $^{235}UC_2$ beads as placed subcutaneously 26 days prior to photograph. Beginning dispersion of the carbon coat shows the microspheres as diffuse rather than discrete particles.

LANL

0005309

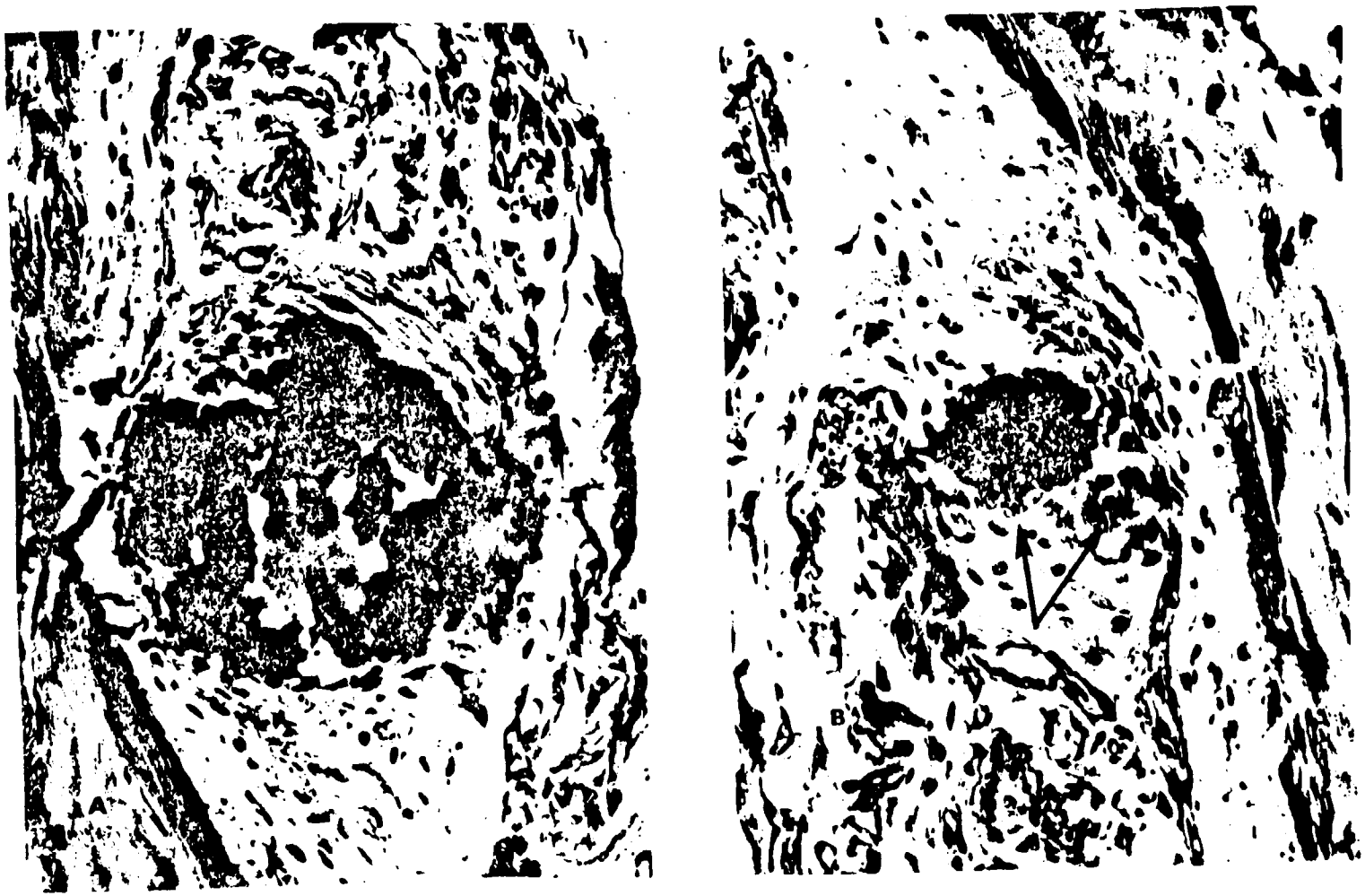

Fig. IV-2. Subcuticular implant of microsphere after 8 weeks. (A) Microscopically, fibrous infiltration of the carbon coat is quite pronounced; and (B) area macrophages are seen to contain large amounts of intracellular carbon.

LANL

0005310

(Fig. IV-2A) and vigorous macrophage ingestion of carbon (Fig. IV-2B). Histologically, total breakdown of the coated spheres had not occurred at 12 weeks, but all were in various stages of disintegration at this time.

Tissue sections from animals sacrificed at intervals showed histological damage to the kidneys, undoubtedly resulting from solubilization of the uranium carbide as the disintegration process proceeds.

Intraperitoneal Implants

Using a suitably sized hypodermic needle and stylet, 5 to 10 carbon-coated $^{235}UC_2$ spheres of uniform size (~150-μ diameter) were placed in the peritoneal cavity of each of 18 rats. Animals were necropsied at 4, 8, 12, and 14 weeks. At 4 weeks all microspheres were recovered essentially intact. Some slight fibrous encapsulation had occurred. At 8 weeks approximately 50 percent of the spheres had disintegrated, resulting in numerous carbon fragments scattered over serosal surfaces and selectively encapsulated. The intact spheres were found encapsulated and adhered to mesenteries and peritoneum (Fig. IV-3A). The capsules were tightly fixed to the particles but could be forcibly removed. On removal, capsules grossly contained carbon fragments. Microscopically, the periphery of the capsules was fibrous connective tissue,

LANL

0005311

Fig. IV-3. Encapsulated microspheres removed from the peritoneum of a rat 8 weeks after implant: (A) gross appearance of capsule, and (B) histosection.

0005312

and many small intracellular carbon fragments could be seen in histiocytes and macrophages (Fig. IV-3B). All spheres placed in the peritoneal cavity had essentially disintegrated by 12 to 14 weeks.

Intraportal Implants

Although intraportal implantation has no direct relation to the practical problem, this site was selected as a means of assuring contact between the particles and the circulation and to observe general foreign body response of another organ. Under nembutal sodium anesthesia, the portal vein of rats was surgically exposed. Four to 8 selected small graphite-coated $^{235}UC_2$ particles were deposited in the portal vein using a properly sized hypodermic needle and stylet. Development of proper technique resulted in minimal bleeding and complete recovery of the majority of animals. Surviving animals were necropsied at 8 and 12 weeks post implant and the liver radiographed for bead location. The liver was then sectioned for histological observations.

After 8 weeks, particles were found lodged in venules in the hepatic mass. Slight fibrous capsules were evident (Fig. IV-4A) with obvious adhesion of fibroblasts to the outer surface of the particle. Histiocytes and macrophages were found to contain many intracellular carbon particles. After

LANL

0005313

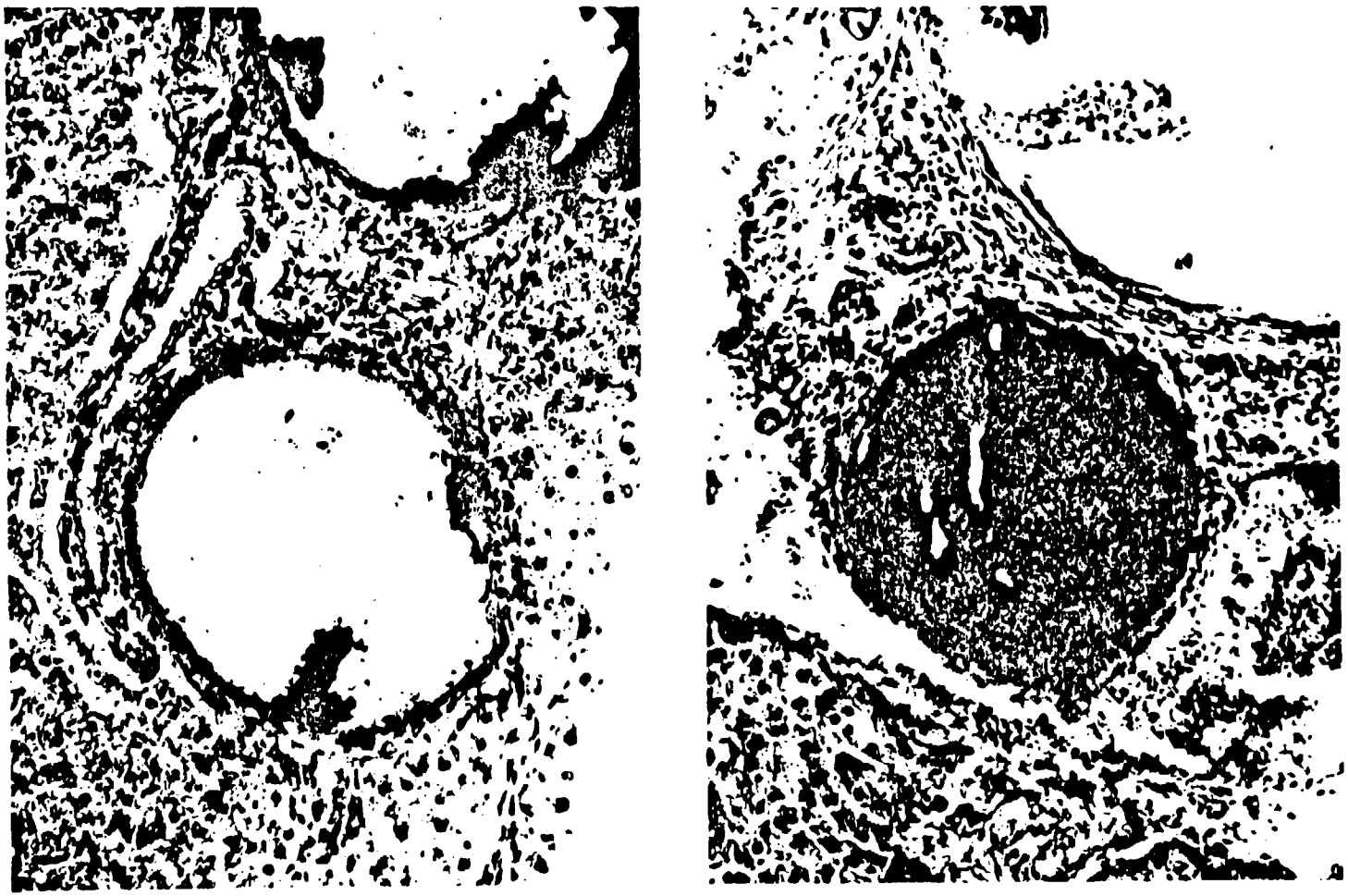

Fig. IV-4. Intraportally implanted microspheres (carbon-coated) after (A) 8 weeks, and (B) 12 weeks in situ. Continued infiltration in this manner ultimately disintegrates the microsphere structure.

LANL

0005314

12 weeks (Fig. IV-4B), fibrous capsules were obviously 2 to 3 times the thickness of the 8-week specimens. Fibrous ingrowths into the mass of the particle were quite pronounced. Some intracellular carbon was seen within cells of the hepatic parenchyma.

Discussion

Although these observations were strictly of an exploratory nature, they support the conclusion that both carbon-coated and uncoated $^{235}UC_2$ microspheres are indeed disintegrated or are even solubilized if placed in contact with interstitial fluids and tissue activity for periods of 8 to 12 weeks. The process of disintegration of the "insoluble" carbon coat by the foreign body reaction is of interest, whereas the relative instability of $^{235}UC_2$ in water leads one to expect rather rapid disintegration of the uncoated spheres and of the coated ones once the integrity of the coating is destroyed.

Histologically, the kidneys of animals with implanted particles show increasing damage, pyknosis of the tubular cells, and severely increased thickening of glomerular epithelium as the period post implant increases. This is easily related histologically to the degree of disintegration of the implanted microsphere.

LANL

0005315

Continued studies are expected to elucidate cellular mechanisms responsible for particle destruction. One could conclude at this point that disintegration is by "piecemeal" destruction and removal of the carbon coat with solubilization of the $^{235}UC_2$ central mass. The rate at which this occurs seems now to be related to the porosity of the sphere or, in the case of the coated ones, to the integrity of the protective carbon coating which may still be seen as insoluble material in cells and interstitial tissue fluids.

LANL

0005316

CHAPTER V

EMERGENT BETA-RAY SPECTRUM OF FISSIONED $^{235}UC_2$ MICROSPHERES AND CALCULATION OF BETA RADIATION DEPTH-DOSE IN TISSUE

(P. N. Dean)

A method has been devised to measure the emergent beta-ray spectrum of small spheres of fissioned $^{235}UC_2$. From this spectrum the beta-ray depth-dose in tissue may be approximated without having to sum the spectra of each fission product or make corrections for self-absorption in the sphere. The gamma response of the detector has been measured and the beta-ray spectrum corrected accordingly. Spectra have been measured at post fission times from 15 minutes to 24 hours using spheres of approximately 150-μ diameter containing about 26 μg of ^{235}U. The integrated beta dose to a 10-μ thick layer of tissue 100 μ below the surface of the skin (assumed to be the average depth of the basal layer) has been calculated for several spheres with diameters ranging from 130 to 160 μ.

LANL

0005317

Methods and Results

The detector used was Pilot B plastic scintillator constructed in such a way that the sphere is completely surrounded by the plastic (Fig. V-1). The detector was coupled to a DuMont 6292 multiplier phototube and a 400-channel pulse-height analyzer. Response of the detector to ^{137}Cs beta rays is shown in Fig. V-2. Beta-ray spectra of several sizes of fissioned spheres both with and without graphite coating have been measured. The rate of decay had to be determined first to permit integration of dose rate to obtain total dose for a given time interval. The primary interest of this experiment was in times from a few minutes to a few hours after fission. Figure V-3 shows the beta-ray spectrum of an 18-μg uncoated microsphere at four times after fission: 26, 85, 140, and 240 minutes. Spectral shape seems quite stable for this time period. Decay was found to obey the following equation for the first 24 hours:

$$y = ct^{-1.115},$$

where y is the count rate at time t minutes, and c is a constant which depends on the initial activity. The neutron flux was approximately 2.0×10^9 neutrons per cm^2-sec, and the irradiation time was 600 seconds. The open circles plotted in Fig. V-3 represent the theoretical shape of the

LANL

0005318

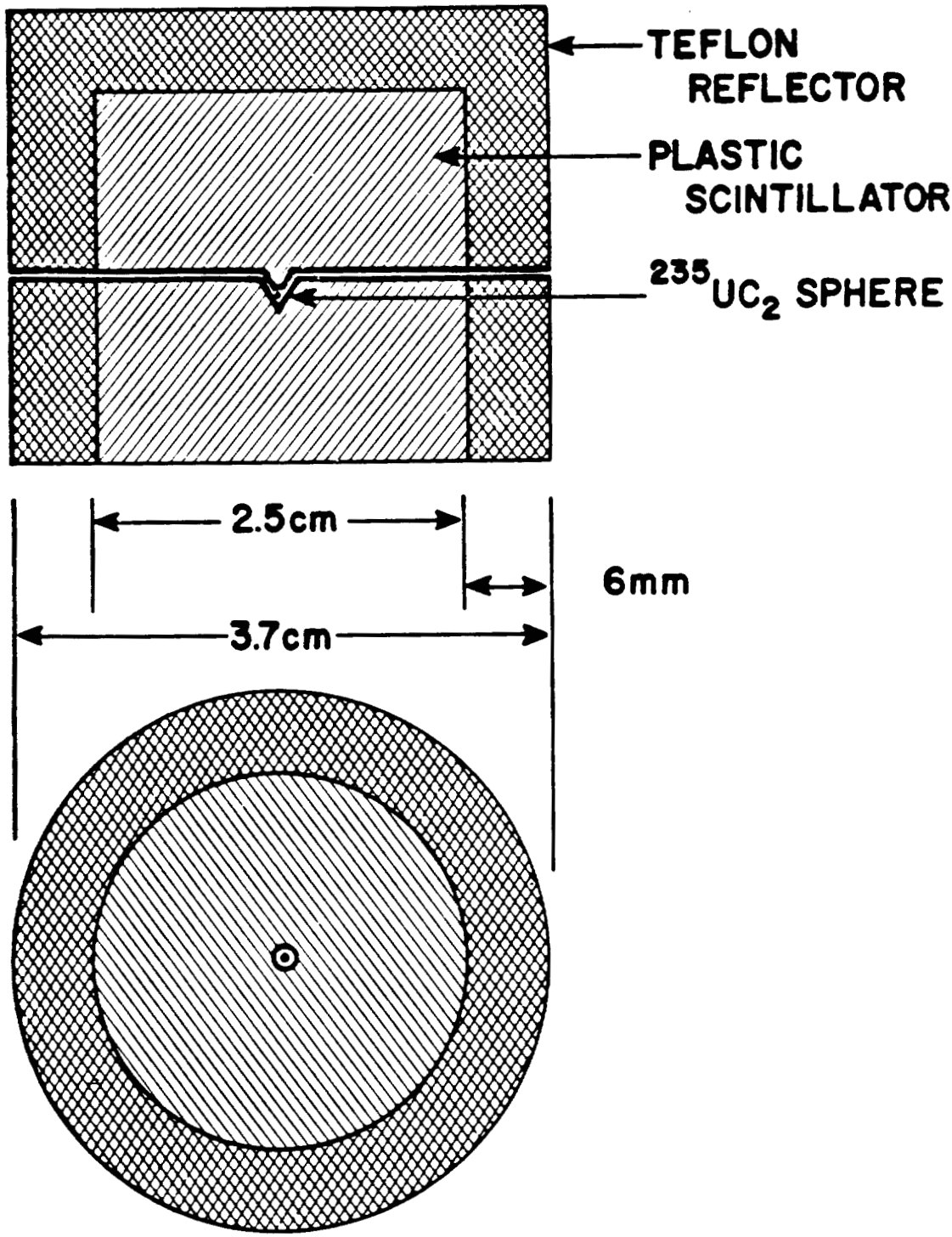

Fig. V-1. Four-pi beta-ray spectrometer.

LANL

0005319

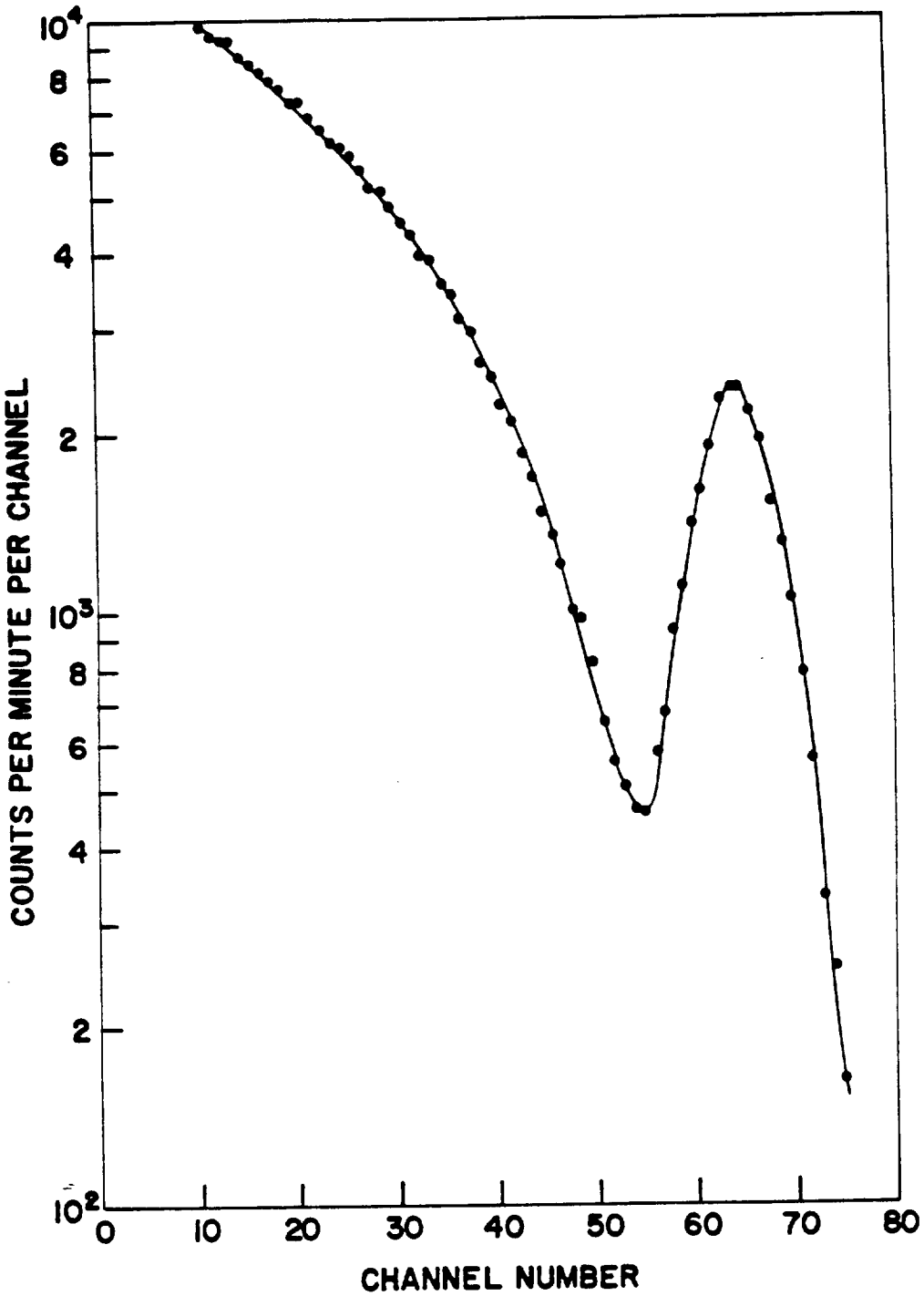

Fig. V-2. Beta-ray spectrum of ^{137}Cs source as measured with a 4π beta-ray spectrometer.

LANL

0005320

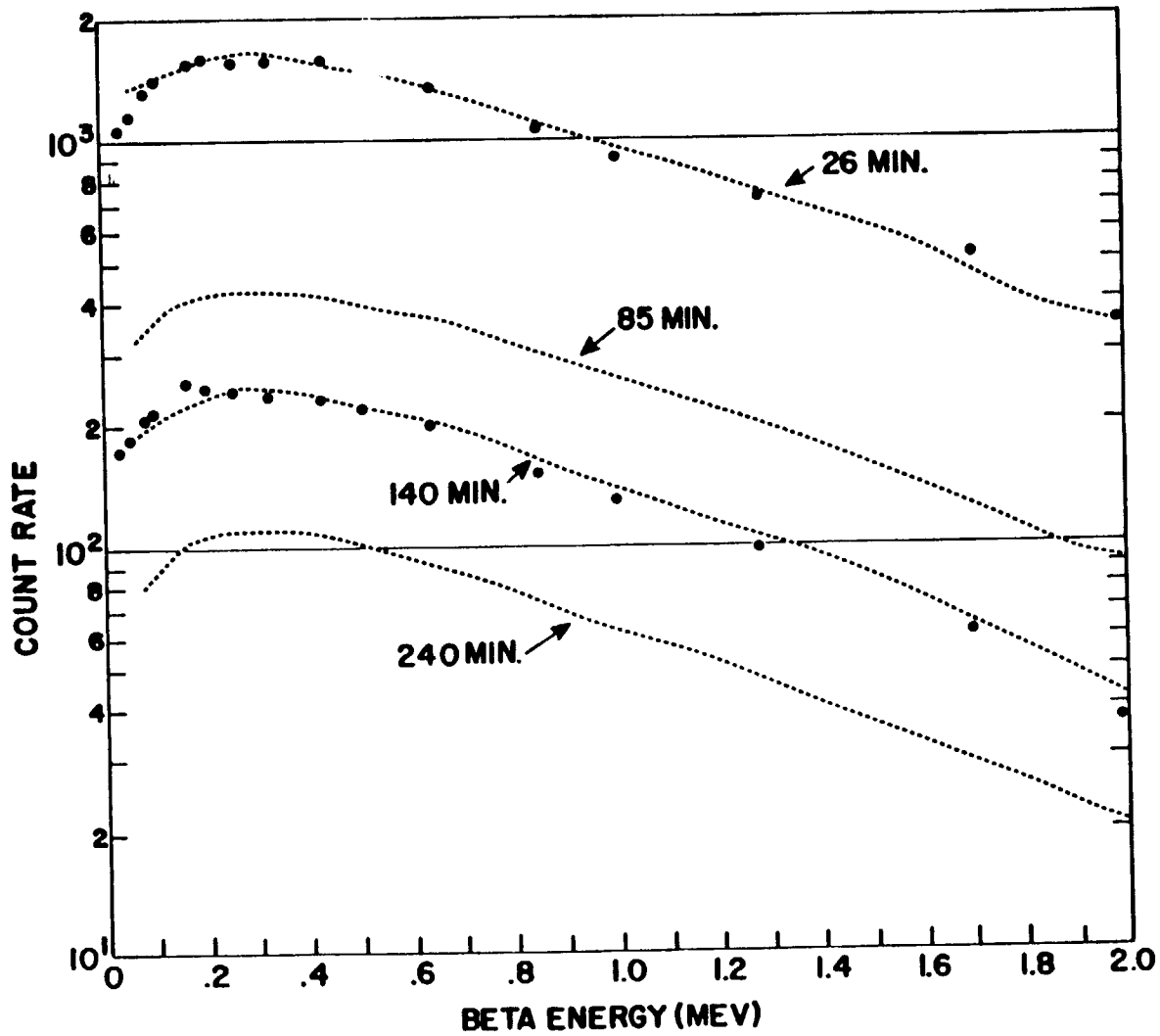

Fig. V-3. Experimental ^{235}U fission product beta decay spectra at four times after fission. The solid points represent the theoretical spectra.

L ANL

0005321

^{235}U fission product beta decay spectra at two different times, as calculated by Nelms and Cooper (1).

Two separate calculations of the dose to a 10-μ thick layer of tissue 100 μ below the surface were made using the energy dissipation distributions of Spencer (2). First, the dose at the surface of the microsphere was calculated using the dE/dx values of Spencer for 100-kev intervals and integrating over the spectrum. Dose at the 10-μ layer was then determined considering a simple exponential absorption. This approximation is useful for distances which are not too large a fraction of the average beta range. The second calculation was made using the spatial distributions of energy transferred to the surrounding material, as calculated by Spencer (2). This calculation takes into account scattering of the electrons and is more rigorous than the exponential absorption method. A comparison of the two methods of calculation is shown in Table V-1. The perpendicular beta-ray depth-dose profile (assuming exponential absorption) was calculated also. Figure V-4 shows the peak dose as a function of depth relative to the dose at 100 μ.

The values given in Table V-1 were part of an experiment to compare dose calculation with measurement using photographic emulsion dosimetry, as described elsewhere in this report. Five carefully sized $^{235}UC_2$ microspheres (coated

LANL

0005322

TABLE V-1. CALCULATED BETA RADIATION DOSES FROM FISSIONED $^{235}UC_2$ MICROSPHERES

Microsphere No.	Average Diameter (μ)	Weight (μg)	Dose (rads)*	
			Exponential Absorption	Spatial Distribution
1	137	14.0	55	66
2	132	14.0	56	66
3	146	19.5	71	83
4	156	20.0	70	83
5	160	21.0	74	86

*Calculated peak dose at 100 μ depth in tissue.

TABLE V-2. CALCULATED BETA RADIATION DOSES FROM FISSIONED $^{235}UC_2$ MICROSPHERES USED IN SKIN EXPOSURE STUDIES

Microsphere No.	Time Interval after Fission (minutes)	Dose (rads)*
1	22 - 268	45,800
2	27 - 274	52,100
3	32 - 278	31,400
4	39 - 279	29,500
5	51 - 283	23,800
6	55 - 284	29,300
7	64 - 286	21,500
8	79 - 287	19,500
9	96 - 288	15,800

*Peak dose at a depth of 100 μ in tissue.

LANL

0005323

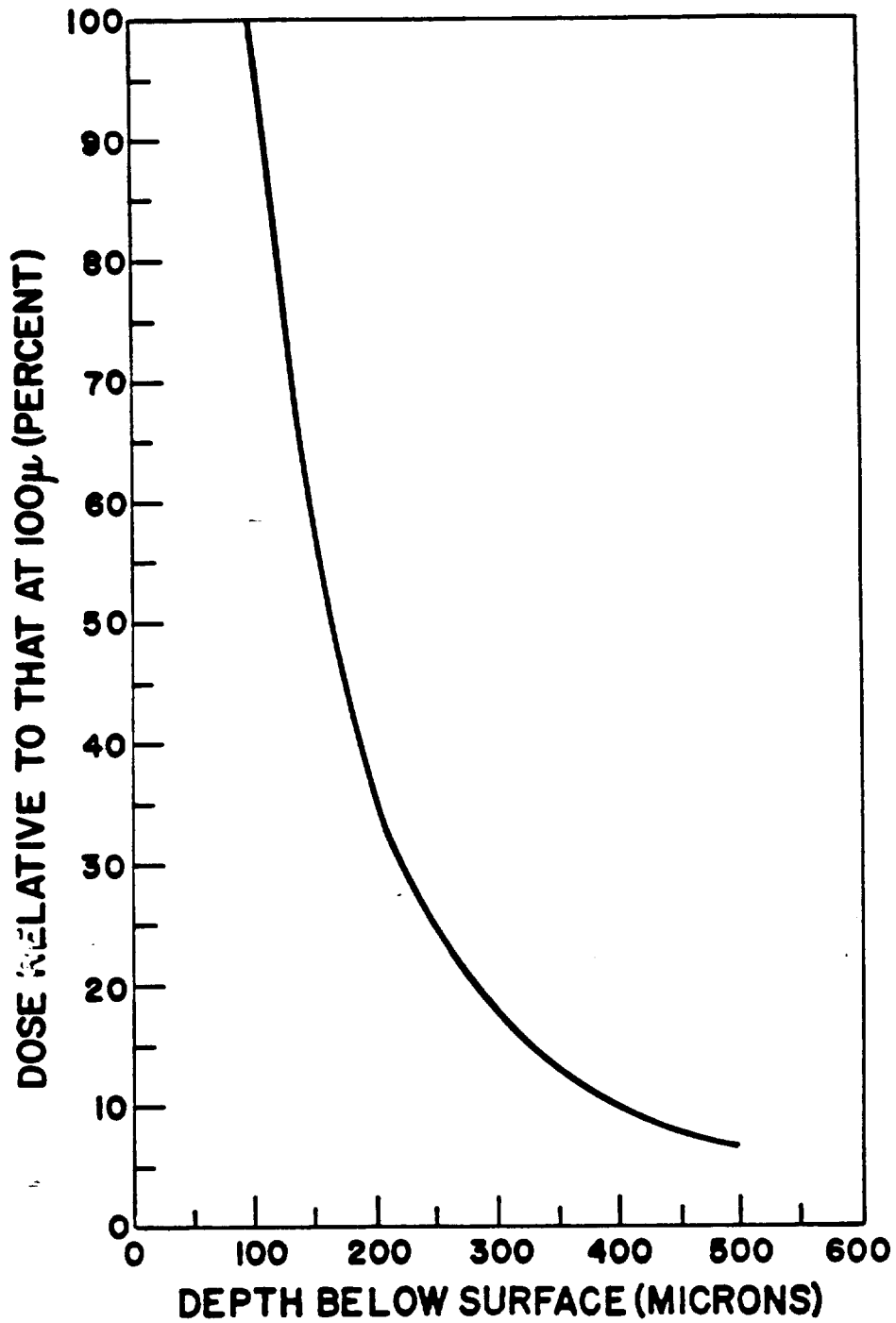

Fig. V-4. Calculated beta radiation depth-dose profile in percent of the dose at a depth of 100 μ, assuming exponential absorption.

LANL

0005324

with a 2-μ thick layer of graphite) were exposed in the thermal column of the Omega East reactor to a flux of about 2.0×10^9 neutrons per cm^2-sec for 600 seconds. The beta spectrum of each microsphere was then measured and peak doses at a depth of 100 μ calculated by the two methods described above. The lateral dose profile in the 10-μ layer of tissue 100 μ below the surface was calculated also, and a comparison of calculation and measurement is shown in Fig. VI-2 of the following chapter.

Another set of spectral measurements and dose calculations was made on activated microspheres used in the skin exposure studies reported in Chapter VII. Those used in the second experiment were exposed in the Omega West reactor to a thermal neutron flux of approximately 2.5×10^{12} neutrons per cm^2-sec for 384 seconds. The microspheres were placed on the skin for different time intervals to vary the dose. Table [illegible] lists the [illegible] intervals and doses calculated by the exponential absorption method.

No attempt has as yet been made to correlate the beta or gamma activity with the number of fissions in the uranium.

REFERENCES

(1) A. T. Nelms and J. W. Cooper, Health Phys. 1, 427 (1959).

(2) L. V. Spencer, National Bureau of Standards Monograph 1 (1959).

LANL

0005325

CHAPTER VI

MEASUREMENT OF BETA-RAY DOSE AT THE AVERAGE DEPTH OF THE BASAL LAYER OF THE SKIN FROM FISSIONED $^{235}UC_2$ MICROSPHERES IN CONTACT WITH THE SKIN SURFACE

(M. A. Van Dilla)

Beta-ray dose distribution to the basal layer (stratum germinativum) of the skin from fissioned $^{235}UC_2$ microspheres in contact with the skin surface was measured experimentally using a mockup. The purpose was to provide dose values independent of the theoretical calculations described in the previous chapter. Since both methods involve a number of simplifications and approximations, it was felt that neither could be relied on alone. The experimental protocol was to expose a set of $^{235}UC_2$ microspheres to a thermal neutron flux of about 2.0×10^9 neutrons per cm^2-sec for 10 minutes and then to measure the dose delivered over a 5-hour period beginning 30 minutes after removal from the reactor. After dose measurement, the electron emission of the microspheres was determined in a scintillation spectrometer to yield data

LANL

0005326

for dose computations. Thus, dose values on the same microspheres were obtained by the two methods.

Methods

The method of dosimetry chosen was photographic emulsion. The emulsion used was Kodak Type NTB, 10 μ thick, on glass slides 1 x 3 x 0.060 in., with protective gelatin coating 0.5 to 1.0 μ thick. This type of emulsion had the best characteristics for beta-ray dosimetry of those investigated by Dudley (1). Although a cellulose acetate film base would have been more tissue-equivalent, this was not available. Calculations of the increase of backscatter due to the higher atomic number glass showed the effect to be small (about 4 percent); it was, therefore, ignored and the easily available glass plates were used.

The method of mocking up the skin and making the exposures is illustrated in Fig. VI-1. The average thickness of the cornified layer of the skin was assumed to be 100 μ, which in the mockup was made up of a 50-μ layer of Mylar film and a 50-μ thickness of double-coated scotch tape. The scotch tape held the microspheres securely and provided good contact with the Mylar film. Good contact between the Mylar film and the emulsion is very important and was accomplished by maintaining a slight negative pressure in the space defined

LANL

0005327

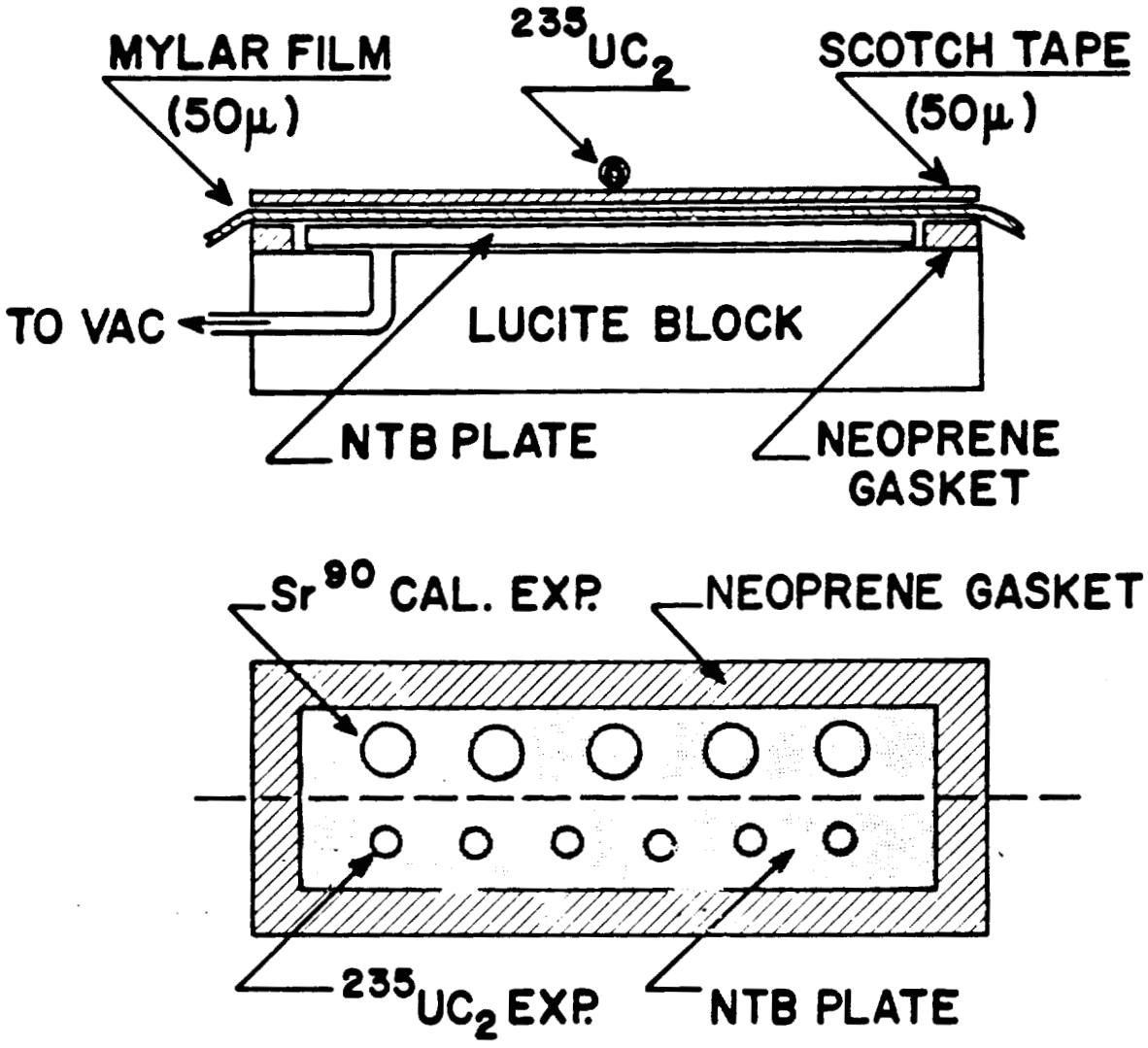

Fig. VI-1. Skin mockup for film dosimetry of $^{235}UC_2$ microspheres. The sphere is stuck to a small square of double-coated scotch tape (50 μ thick) which, in turn, is stuck to Mylar film surface, providing a simulated 100-μ thick "cornified" layer.

LANL

0005328

by the Lucite block, neoprene gasket, and Mylar film. The Lucite block simulated the deeper underlying tissues.

Half of the NTB plate was used for microsphere exposure; 5 to 6 microspheres at approximately 0.5-in. intervals were usually used. The other half of the plate was used as a ^{90}Sr beta-ray standardization strip similar to that proposed by Dudley (1), the maximum specific activity being about 640 μc per gram. All plates were exposed to the ^{90}Sr standardization source for 15 minutes, providing a constant exposure to check reproducibility of development procedures and emulsion characteristics. The development procedure was 2 minutes in Kodak developer D-19 at 68°F, 10 minutes in acid fixer, 5 minutes in hypo to clear, and 10 minutes wash.

Measurement of emulsion density was done with an Eastman microdensitometer; the size of the scanning spot was about 25 x 25 μ. Conversion of density to dose was accomplished by calibration exposures in a ^{60}Co gamma-ray field accurately calibrated for air dose; 0.90 rad per roentgen was used to convert from air dose to absorbed dose in the emulsion.

Results

Figure VI-2 shows a comparison of measured and calculated lateral dose distribution at 100 μ beneath the surface from one of the microspheres. The dose distribution is very narrow, the width at half-maximum being 400 μ, or 2-1/2 times the

LANL

0005329

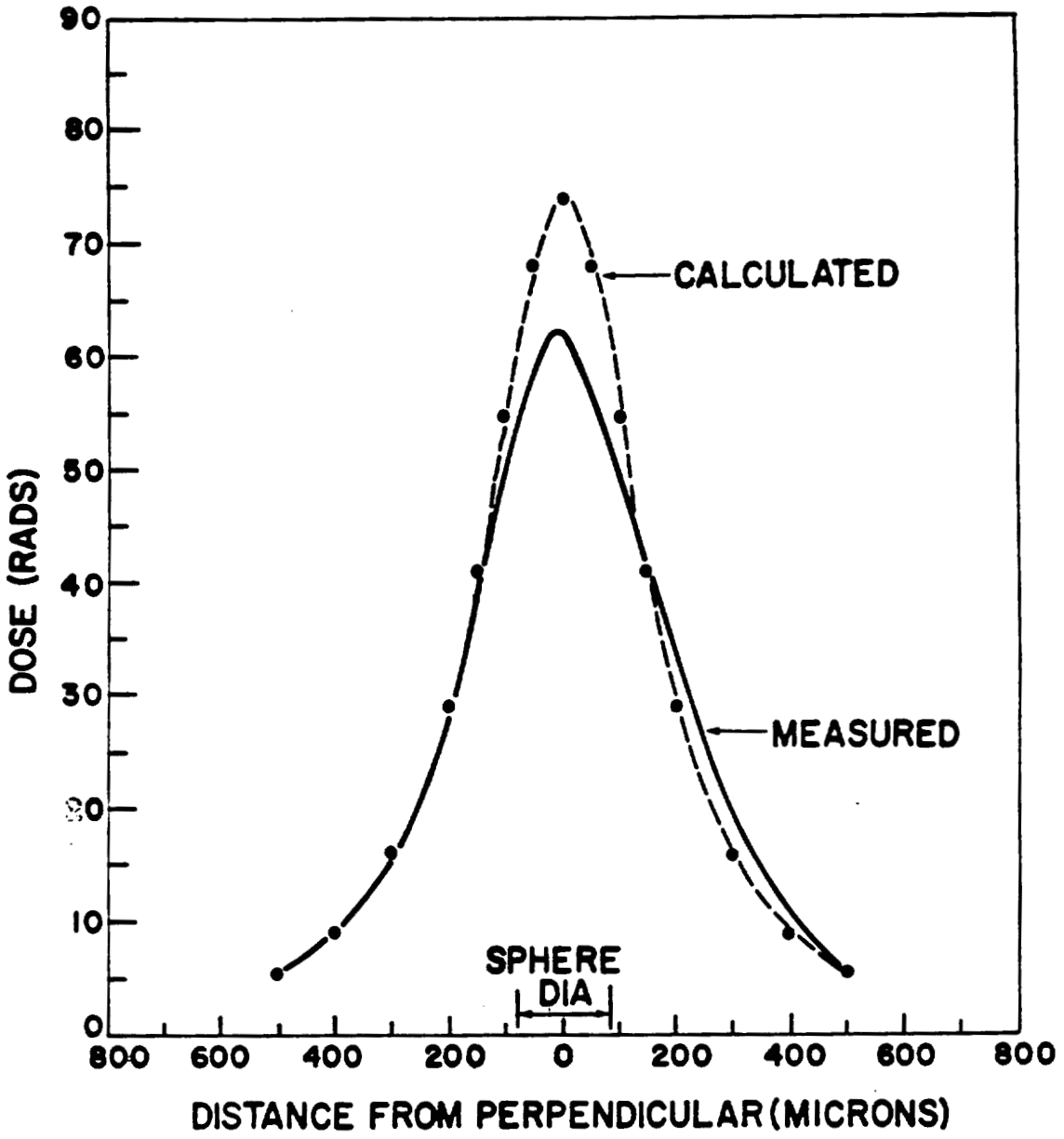

Fig. VI-2. Measured and calculated lateral beta-ray dose distribution at 100 μ below the surface from an activated $^{235}UC_2$ microsphere (160 μ in diameter).

LANL

0005330

microsphere diameter. Thus, the dose is confined mainly to a very small area of basal layer (about 1 mm^2). The dose distribution was not quite symmetrical for 3 of the 5 microspheres measured (as the data for No. 6 in Fig. VI-2 show) but was symmetrical for the remaining 2 beads. Asymmetry may be experimental error in the film dosimetry method or may possibly be due to departures of the microspheres from sphericity.

Table VI-1 shows a comparison of calculated and experimentally measured peak dose values for 5 activated spheres. The simpler of the theoretical approaches (assuming exponential absorption) yields peak doses which are 20 percent larger than the measured values on the average, while the second theoretical approach yields results about 20 percent larger than the first. Considering the many approximations and sources of error inherent in these methods, the discrepancies are not surprising. Compared with the variability of the biological response, however, these discrepancies are probably small and of little significance.

REFERENCES

(1) R. A. Dudley, Nucleonics 12(5), 24 (1954).

(2) L. V. Spencer, National Bureau of Standards Monograph 1 (1959).

0005331

TABLE VI-1. CALCULATED AND MEASURED BETA RADIATION DOSE FROM ACTIVATED $^{235}UC_2$ MICROSPHERES[a]

Microsphere No.	Diameter (μ)	Weight (μg)	Peak Dose (rads) 100 μ beneath Surface		
			Film	Theoretical[b]	Theoretical[c]
1	137	14.0	43	55	66
2	132	14.0	44	56	66
4	146	19.5	52	71	83
5	156	20.0	60	70	83
6	160	21.0	62	74	86

[a]Exposed to a thermal neutron flux of 1.99×10^9 neutrons per cm^2-sec for 10 minutes and measured over a 5-hour period, beginning 32 minutes after removal from the reactor.

[b]Assumes exponential absorption.

[c]Uses energy deposition data of Spencer (2).

LANL

0005332

CHAPTER VII

OBSERVATIONS OF ACUTE RADIATION EFFECTS FROM FISSIONED $^{235}UC_2$ MICROSPHERES IN CONTACT WITH THE SKIN SURFACE

(J. C. Hensley, W. H. Langham, and P. N. Dean)

Whether control of reentry particle size can provide a worthwhile means of reducing the potential hazards from space applications of nuclear power sources may depend on the seriousness of the lesions resulting from contact of such particles with the skin surface. Simulated exposures which may be incurred upon reentry of fissioned $^{235}UC_2$ microspheres (size range of 100 to 200 μ) have been carried out on the backs of monkeys to observe the magnitude and extent of the acute effect in relation to the calculated beta radiation dose at the average depth of the basal layer of the skin.

Methods

Histological examination of the skin of the back of the Macaca speciosa monkey showed similarity in thickness and

LANL

0005333

structure to that of man, especially the skin of the plantar or dorsal forearm surface. Since pronounced cutaneous structural differences exist among human subjects, both among individuals and between different areas on the same individual, it was felt that the skin on the back of the monkey simulated human skin adequately for preliminary observations.

The $^{235}UC_2$ microspheres used were the same as those on which spectral measurements were made for the dose calculations reported in Table V-2 (Chapter V). They were uncoated and in the size range of 140 to 160 μ in diameter. As soon as possible after activation in the Omega West reactor (see Chapter V), the microspheres were placed on the skin surface in the grid areas on the backs of the animals. They were fixed in place with a light coat (15- to 18-μ thickness) of protective spray bandage (Mycodex) by first applying the spray and firmly pressing the bead into the coating before it had completely set. After placement the spheres were covered by 1-cm hemispherical lead cups for protection of the operator during subsequent placements.

Dose was calculated from spectral measurements, time of placement, and interval of contact as described in Chapter V.

Two experiments were carried out: the first covered the dose range of from 1300 to 10,000 rads, and the second covered the dose range of from 16,000 to 52,000 rads (calculated). Specific dose information and grid identification

LANL

0005334

numbers are given in Table VII-1. Microsphere placement and the tatooed grid system used to delineate and to identify the individual exposure areas are illustrated in Fig. VII-1. After exposure the animals were observed daily and the individual implant sites inspected for gross characteristics and time of appearance of lesions. A weekly photographic record (both color and black and white) of the more prominent lesions (second experiment) was made through the fourth week. At 5 weeks full-thickness skin biopsies were taken of representative high- and low-dose exposure areas. Observation of the remaining exposed areas is continuing.

Results

Gross Observations (First Experiment)--Immediately after exposure all sites (1270 to 9600 rads) seemed to show a slight erythema which, at the highest doses, was about 2- to 3-mm in diameter. Twenty-four hours post exposure, erythema was discernible only at the three highest doses (Table VII-1). At 48 hours only the highest dose lesion was visible grossly, showing a slight erythema 1- to 2-mm in diameter.

Five days post exposure slight erythema was visible at the sites exposed to 9600 and 8900 rads. This was transient, and at 14 days no evidence of exposure was visible grossly.

LANL

0005335

TABLE VII-1. ESTIMATED BETA RADIATION DOSES TO BASAL LAYER OF THE SKIN (100 μ IN DEPTH) FROM FISSIONED $^{235}UC_2$ MICROSPHERES

Grid No.	Calculated Dose[a] (rads)	Dose Derived from Measurement[b] (rads)
First Experiment		
2-2	9600	7680
2-6	8900	7120
2-14	7500	6000
2-17	7040	5630
4-2	5900	4720
4-6	5400	4320
4-10	4860	3890
4-14	4520	3620
4-17	4080	3260
6-2	3380	2700
6-6	2760	2210
6-10	2020	1620
6-14	1270	1020
Second Experiment		
1-6	52,100	41,700
1-1	45,800	36,600
1-12	31,400	25,100
1-16	29,500	23,600
3-13	29,300	23,400
3-3	23,800	19,000
5-1	21,500	17,200
5-5	19,500	15,600
5-16	15,800	12,600

[a]Peak dose calculated assuming exponential absorption.

[b]Eighty percent of calculated peak dose (see Chapter VI).

LANL

0005336

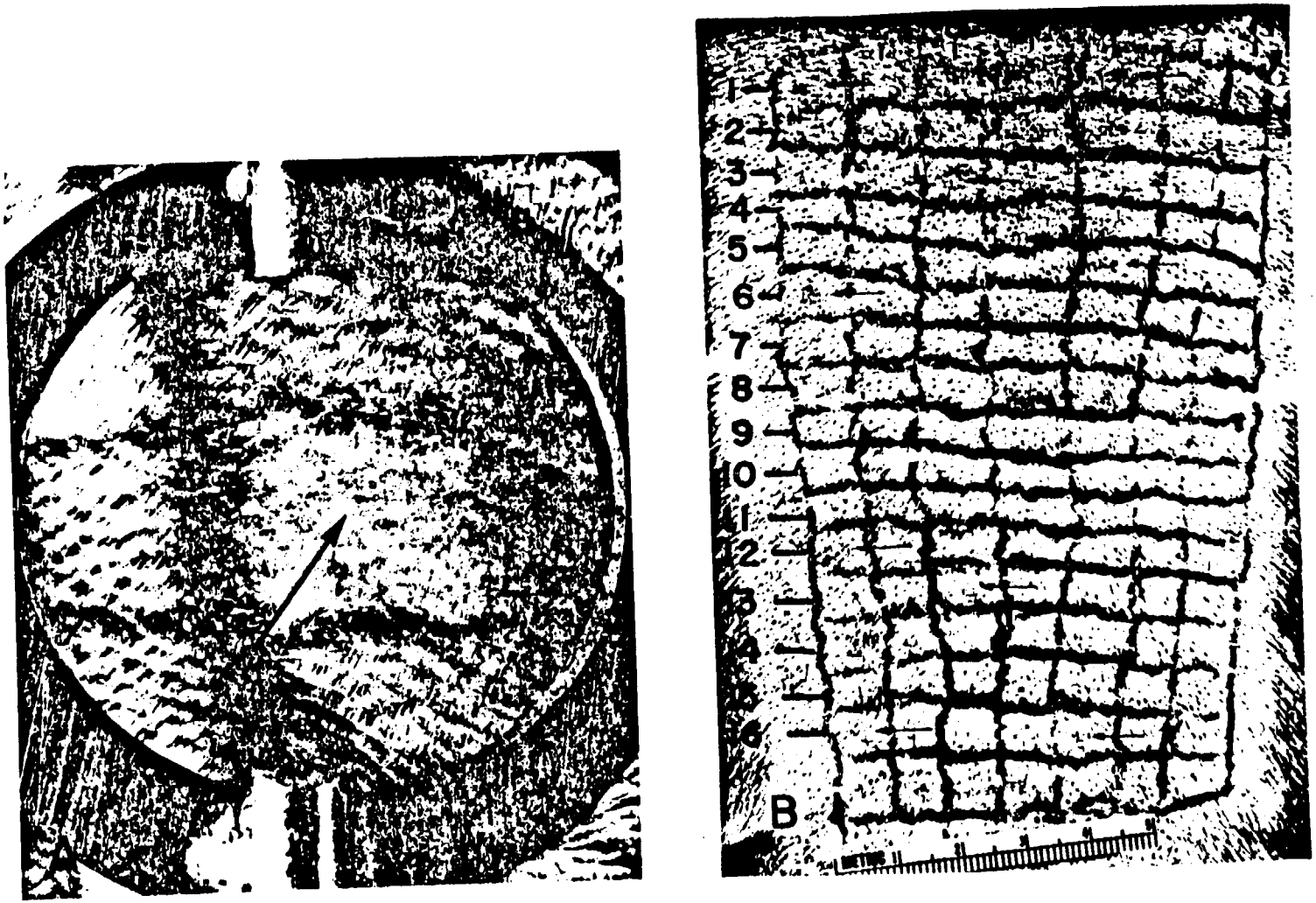

Fig. VII-1. Method of placing microspheres (A), and exposure grid system (B). This is a picture of the back of the animal used in the second experiment 7 days after exposure. Arrows point to the exposed areas.

LANL

0005337

A palpable induration 2- to 3-mm in diameter was noted at the highest dose site. At 26 days all visible or palpable evidence of exposure was negative to gross examination.

Gross Observations (Second Experiment)--The second experiment involved exposures to calculated doses of from 15,800 to 52,100 rads. Immediately after exposure all sites showed a diffuse erythema, which may have been augmented by backscatter from the hemispherical lead shield placed over each microsphere to protect the operator. At 48 hours erythema was visible at all sites but was much more discrete than was the case immediately post exposure.

At 72 hours elevation of the stratum corneum was apparent at the sites of the two highest doses. At this time liquefaction of the stratum lucidum and Malphigian stratum was suspected, and the formation of a tiny, shallow vesicle was apparent at the highest dose.

Beyond about 72 hours it was not possible to distinguish definitive gross qualitative differences in the lesions as a function of exposure dose (particularly those above about 25,000 rads). This could be due largely to microscopic variations in skin structure even within a grossly uniform area such as the back. Figure VII-1B shows the whole back of the animal 7 days post exposure. Arrows point to the exposure sites. Only a few of the lesions are barely visible at this

LANL

0005338

magnification in black and white reproduction. Color photographs, however, showed small areas of erythema (3- to 5-mm in diameter) at all dose levels, which persisted through the 21st day.

Only the lesion produced by the highest dose is used to describe the sequential epidermal reaction, since gross dose-effect differences (particularly at the higher doses) were not distinguishable. Figure VII-2 shows the 52,100-rad lesion at 7, 14, 21, and 28 days post exposure insofar as it can be shown by black and white reproduction. The color photographic record afforded much better delineation and detail. Several other lesions appeared quite similar to this one, particularly those resulting from exposures above about 25,000 rads. Seven days post exposure, vesiculation was reduced, and rupture of the stratum corneum produced the micro-lesion seen in Fig. VII-2A. Two weeks post exposure the reaction (Fig. VII-2B) was reduced to a moderate hyperemia with considerable subsurface induration. Twenty-one days after exposure (Fig. VII-2C) the gross lesion had regressed to a diameter of about 3 mm with increased induration. At 28 days shallow, dry desquamation had resulted (Fig. VII-2D) which regressed to virtually visible normalcy by 36 days after exposure. At this time, however, discrete induration was palpable at the five highest dose sites.

LANL

0005339

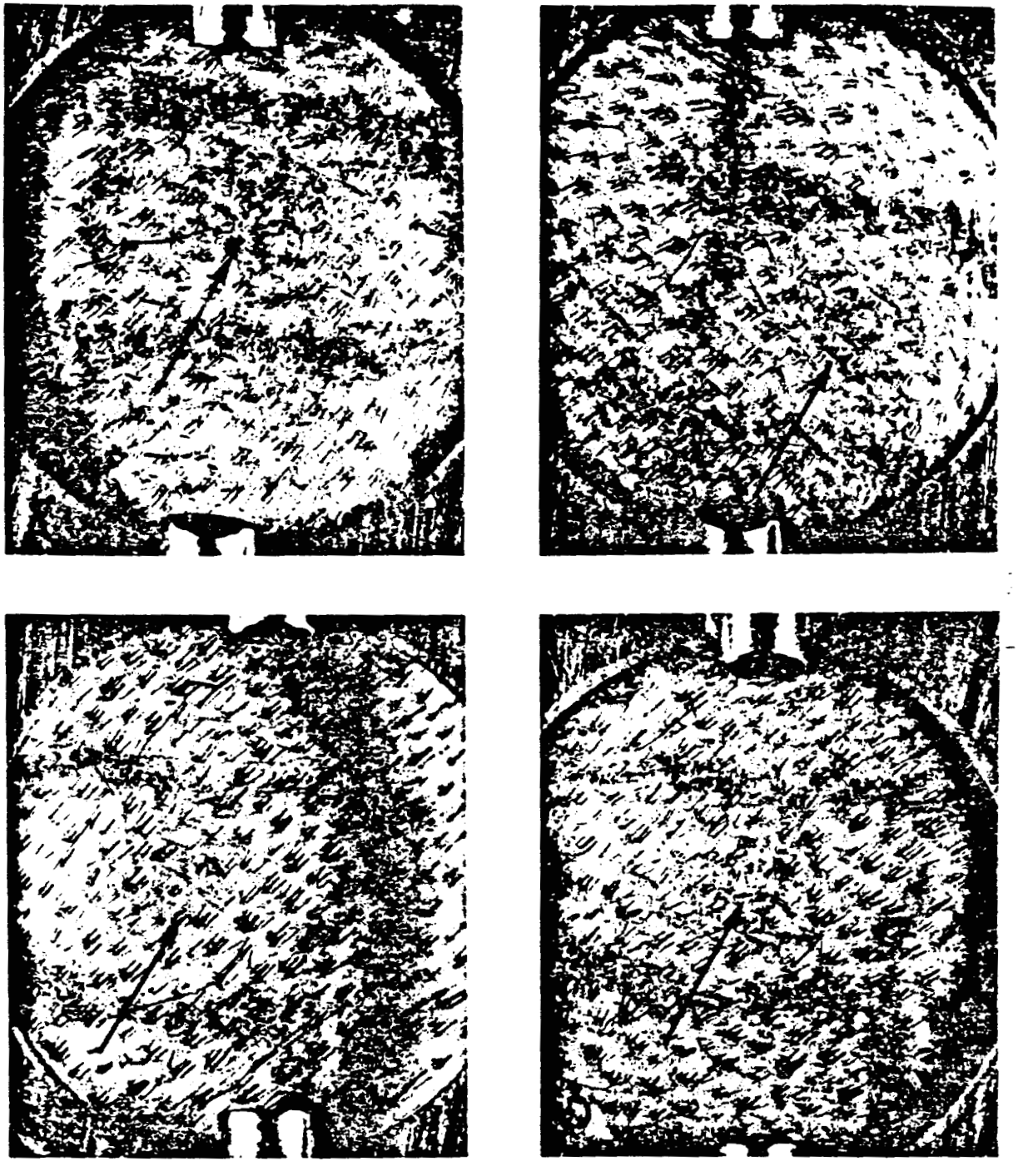

Fig. VII-2. Pictorial record of the 52,100-rad lesion at (A) 7 days, (B) 14 days, (C) 21 days, and (D) 28 days post exposure.

0005340

Consequently, biopsy material was taken at this time for histopathological study. Ninety days post exposure no lesions were visible or palpable at any of the remaining sites.

Microscopic Observations--Microscopically, the 52,100-rad lesion (6 weeks post exposure) appears chiefly as an epithelial lesion consisting of a decreased number of epithelial nuclei separated by variable but larger than normal amounts of eosinophilic keratinized cytoplasm. Some of the basal cells show nuclear pyknosis and vacuolation, but the majority have become metaplastic squamous cells with well developed intercellular bridges. Mitotic activity is absent. Other areas but a few microns away show pronounced basal cell hyperplasia without cytoplasmic change. Acanthosis, dyskeratosis, and parakeratosis are the predominant features of the stratum corneum which is thinner than normal. The site of the 29,300-rad exposure at 6 weeks shows similar features. Lesions at both doses show edema of the loose perivascular areolar tissues of the outer dermis. Lymphocytic infiltration of this areolar tissue is present as in chronic inflammation. Hair follicles and dermal glands show slight atrophy and increased pigmentation. Necrotic lymphocytic nuclear debris is present among the inflammatory cell exudates. These dermal changes are not inconsistent with the depth-dose distribution, since the beta dose at 500 μ

LANL

0005341

is about 6 percent of the dose at the depth of the basal layer (Fig. V-4).

Biopsy material from the 9600-rad site, taken at 90 days post exposure, microscopically shows basal cell hyperplasia and persistence of squamous nuclear gigantism, dyskeratosis, and dysplasia in the epidermis. In the dermis, complete follicular atrophy has transpired, with loss of all accessory structures except the radioresistant smooth muscle bundles of the arrectores pilorum. The chronic inflammation and edema have disappeared. Ulceration and dermal necrosis were never seen. Dermal repair by fibroplasia was, therefore, absent.

The conclusion that these lesions are of inconsequential medical nature would seem to be supported firmly by: (a) the failure of epithelial ulceration and dermal necrosis to occur; (b) the absence of repair by fibrosis; (c) the absence of degenerative sclerotic changes in the dermal collagen; and (d) the rapid replacement of the irradiated dysplastic epithelium by adjacent normal basal cells and their squamous progeny.

Discussion

Studies thus far indicate too great a variation in local tissue reaction to permit any quantitative evaluation

LANL

0005342

of a gross dose-response relationship for pinpoint exposures of the epidermis. It is expected that histological studies will show this variation to be due to the variety of microscopic structural features over which a microsphere may be placed. Proximity of sebaceous glands, sudoriferous glands, hair follicles, circulatory elements, etc., may influence response to a given exposure dose. Serial histological studies will probably have to be resorted to for refined quantitative dose-response definition. Further histopathological studies should also qualify the nature of the gross reactions seen to date.

Due to the small (100- to 200-μ) size of the exposure sources, lesions produced by high total-dose exposures were remarkably small. At no time was any lesion, whether hyperemia or swelling of inflammation, in excess of about 5 mm in diameter. As would be expected from the limited range of the beta rays, grossly the lesions appeared quite shallow. Histological examination of biopsy material, however, showed radiation changes in dermal structures. It appears from these preliminary observations that repair of the epidermis is complete and that the small lesions are self-limiting. With doses below about 10,000 rads the effects should be negligible as concerns the general health of man or beast when confined to a few such exposures on cutaneous surfaces.

LANL

0005343